Laura Tillikainen and Sami Siljamäki. 2008. A multiple-source photon beam model and its commissioning process for VMC++ Monte Carlo code. In: Frank Verhaegen and Jan Seuntjens (editors). Proceedings of the Third McGill International Workshop on Monte Carlo Techniques in Radiotherapy Delivery and Verification. Montréal, Canada. 29 May - 1 June 2007. Journal of Physics: Conference Series, volume 102, number 1, 012024.

http://www.iop.org/journals/jpcs
http://stacks.iop.org/jpcs/102/012024

Journal of Physics: Conference Series **102** (2008) 012024 doi:10.1088/1742-6596/102/1/012024

A multiple-source photon beam model and its commissioning process for VMC++ Monte Carlo code

Laura Tillikainen and Sami Siljamäki

Varian Medical Systems Finland Oy, Paciuksenkatu 21, FIN-00270, Helsinki, Finland

E-mail: laura.tillikainen@varian.com

Abstract. The use of Monte Carlo methods in photon beam treatment planning is becoming feasible due to advances in hardware and algorithms. However, a major challenge is the modeling of the radiation produced by individual linear accelerators. Monte Carlo simulation through the accelerator head or a parameterized source model may be used for this purpose. In this work, the latter approach was chosen due to larger flexibility and smaller amount of required information about the accelerator composition. The source model used includes sub-sources for primary photons emerging from target, extra-focal photons, and electron contamination. The free model parameters were derived by minimizing an objective function measuring deviations between pencil-beam-kernel based dose calculations and measurements. The output of the source model was then used as input for the VMC++ code, which was used to transport the particles through the accessory modules and the patient. To verify the procedure, VMC++ calculations were compared to measurements for open, wedged, and irregular MLC-shaped fields for 6MV and 15MV beams. The observed discrepancies were mostly within 2%, 2 mm. This work demonstrates that the developed procedure could, in the future, be used to commission the VMC++ algorithm for clinical use in a hospital.

1. Introduction

Monte Carlo (MC) based methods are widely recognized to be the most accurate dose calculation algorithms currently available. They are superior over other commonly used methods especially near the boundaries of materials with different electron densities, and in complex treatment geometries. Another significant benefit over other methods is that the MC calculation time is roughly independent of the number of fields in a treatment plan, but depends only on the size of the volume of interest and required statistical accuracy. Until recently, long calculation times required to achieve acceptable statistical accuracy have limited the use of MC techniques for clinical photon beam treatment planning. However, due to recent advances in variance reduction techniques [1, 2] and computer technology, MC techniques are starting to become feasible also there.

A major challenge for adopting MC to clinical use is the modeling of radiation output of the linear accelerator. The beam properties may differ between individual accelerators even of the same manufacturer and model. Full simulation through the accelerator head is possible, but it requires detailed knowledge of the accelerator composition [3]. Often all relevant parameters are not known with sufficient accuracy, and thus a time-consuming tuning of e.g. the electron beam

spot size and energy must be performed [4]. Even with such tuning, sufficient accuracy may not be reached due to limited degrees of freedom in the model. Another approach is to use a simpler multiple-source model (MSM) to describe the accelerator output [5, 6]. These models contain physical parameters that can be tuned to match measurements, or alternatively the parameters can be fitted to MC-simulated phase-space data. In this work, the MSM approach was used together with an automatic process to optimize the free model parameters based on standard beam data measurements [7]. The output of this optimized MSM was then used as input for the VMC++ code [1, 2] to transport the particles through static accessory modules (e.g. wedges and the MLC) and through the patient. With this approach, e.g. the tongue-and-groove effect can be accurately modeled without increasing the calculation time considerably. The source model was originally designed for the AAA superposition/convolution algorithm (Eclipse$^{\text{TM}}$ Integrated Treatment Planning System, Varian Medical Systems Inc., Palo Alto, CA). Modifications made to incorporate the model with a MC-based algorithm are described in Section 2. The process was tested by comparing measured and calculated open fields, wedged fields and irregular MLC apertures for 6MV and 15MV photon beams for a Varian 2100 C/D accelerator. The results are presented in Section 3.

2. Materials and methods

There are three phases in the developed calculation process: (1) sampling of particles from the MSM, (2) transport of the particles through the static accessory modules, and (3) transport through the patient geometry defined by the CT-image. Between phases (1) and (2), the particles sampled from the MSM are projected to the starting plane of the topmost accessory according to their initial position and direction. Similarly, between phases (2) and (3), the particles from the last accessory module are projected to the patient surface.

2.1. The multiple-source model and optimization of the free model parameters

The MSM used in this work includes three sub-sources: primary photon source, extra-focal photon source, and electron contamination source. The free parameters of the model were derived using the optimization procedure presented in Ref. [7]. The free parameters $\bar{E}(r)$ and $I(r)$ describe the mean radial energy and the intensity profile for the primary photon source, w_{ef}, σ_{ef}, $\bar{E}_{\text{ef}}$ are the weight, size and mean energy for the extra-focal photon source, $\sigma_{\text{e},i}$ $(i = 1, 2)$ are the sigmas of the two Gaussians for the electron contamination source, c is the weight of the first Gaussian, and $w_{\text{e},i}$ $(i = 1, \ldots, 6)$ are the weights that determine the empirical electron contamination curve via $c_{\text{e}}(z) = \sum_{i=1}^{6} w_{\text{e},i} \exp(-k_i z)$. See table 1 in Ref. [7] for a detailed description of the parameters. The optimization procedure minimizes an objective function measuring deviations between measurements and calculations, and simultaneously restricts the parameters into a physical range using heuristic penalty terms. During the optimization, the dose is calculated using a fast pencil-beam-kernel based method.

2.2. Absolute dose calibration

VMC++ calculates dose in units of Gy/particle. To convert this to Gy/Monitor Unit (MU), we calculate the dose with VMC++ in the calibration geometry where the Gy/MU ratio is known to be $\text{Gy}_{\text{calib}}/\text{MU}_{\text{calib}}$. Then a conversion factor c_{F} (particles/MU) is computed as $c_{\text{F}} = (1/d_{\text{ref}}) \times (\text{Gy}_{\text{calib}}/\text{MU}_{\text{calib}})$, where d_{ref} is the dose per particle calculated in the calibration geometry. The calculated dose distribution is smoothed with a 3D-Gaussian filter before determining d_{ref}.

2.3. Determination of sub-source weights

Since the weights of the sub-sources in the original model are defined as fractions of deposited energy, they must be converted to fractions of emitted particles for MC calculation. This

is accomplished in the following way. For each sub-source i, the particle weight $w_{i,\mathrm{p}}$ can be calculated from the energy weight $w_{i,\mathrm{energy}}$ using formula

$$w_{i,\mathrm{p}} = w_{i,\mathrm{energy}} \int_S \Phi_{i,\mathrm{p}}(\vec{s})\ \mathrm{d}\vec{s}, \tag{1}$$

where $\Phi_{i,p}$ is the particle fluence [1/m^2] for sub-source i obtained from the MSM, $\vec{s}$ is a 2D vector in a plane, and S defines the surface from which particles are sampled. For the primary photon source, $w_{\mathrm{prim,energy}} = 1$, $\Phi_{\mathrm{prim,p}}(x, y) = I(x, y)/\bar{E}(x, y)$ and the integration goes over a rectangle defined by current jaw positions.

For the extra-focal source, the polar direction angle ϕ is assumed to follow a cosine distribution, and the azimuthal direction angle θ is assumed to follow a uniform $[0, 2\pi]$ distribution. Hence, for the energy fluence for a single extra-focal source point, it holds $\Phi_{\mathrm{ef,energy}}(\phi) \propto \cos(\phi)$, and for the particle fluence $\Phi_{\mathrm{ef,p}}(\phi) \propto \cos(\phi)/\bar{E}_{\mathrm{ef}}$. At infinite distance the Gaussian source reduces to a point source, and a simple integration in spherical coordinates can be performed. The maximum polar angle, $\phi_{\max}$, can be determined from the jaw opening.

Since the original source model does not contain a weight $w_{\mathrm{el,energy}}$ or spectrum $S_{\mathrm{el}}(E)$ for the contamination electrons, these parameters must be determined from the empirical curve $c_{\mathrm{e}}(z)$. The spectrum is determined by first selecting a template spectrum (available for 6, 10 and 15 MV) simulated with BEAMnrc, which has a nominal energy closest to the current beam. Then the energy axis of the template spectrum is scaled by a factor that minimizes the difference between $c_e(z)$ and calculated electron depth dose curve, which is computed based on the current spectrum and pre-calculated mono-energetic electron depth dose curves. The weight $w_{\mathrm{el,energy}}$ is obtained by integrating $c_{\mathrm{e}}(z)$ along the z-direction, and normalizing the result with the total energy of each MC simulated pencil-beam-kernel used in AAA. Then the particle weight $w_{\mathrm{el,p}}$ can be obtained by setting $\Phi_{\mathrm{el,p}}(x, y) = I(x, y)/\bar{E}_{\mathrm{el}}$, and integrating over the rectangle defined by the current jaw positions. $\bar{E}_{\mathrm{el}}$ is the mean energy of the contamination electrons calculated from the spectrum $S_{\mathrm{el}}(E)$.

2.4. Sampling of particles

For each particle sampled from the source model, one needs to determine an initial position ($\vec{x}$), direction ($\vec{d}$), energy (E), and particle type (photon or electron). The sampling proceeds by first selecting the sub-source for the current particle based on the respective sub-source weights $w_{i,\mathrm{p}}$.

For the *primary photon source*, a position (x, y) at isocenter plane is uniformly sampled from a rectangle defined by the jaw positions. Then the rejection sampling technique is used to account for the particle fluence profile $\Phi_{\mathrm{prim,p}}(x, y)$: First a random number r is sampled from a uniform [0,1] distribution. If $r > \Phi(x, y)/\Phi_{\max}$, the particle is rejected and the sampling process is repeated — otherwise the particle is accepted. Then the particle is projected to the topmost accessory plane according to a direction vector from the target to the point (x, y, z_{SAD}), where z_{SAD} is the source-to-axis distance. Energy E is sampled from the radial spectrum $S(E, r)$ using a histogram sampling technique.

For the *extra-focal photon source*, a position (x, y) at the source plane located at a distance z_{ef} from target is sampled from a 2D-Gaussian distribution with the standard deviation of σ_{ef}. The sampling is iterated until $|x|, |y| < 3\sigma_{\mathrm{ef}}$. The direction vector $\vec{d}$ is obtained by sampling the azimuthal direction angle θ from a uniform [0, 2π] distribution, and the polar direction angle ϕ from a cosine distribution. Then the particle is projected from point (x, y, z_{ef}) along direction $\vec{d}$ to the topmost accessory plane. Energy E is then sampled from the extra-focal photon spectrum $S_{\mathrm{ef}}(E)$ using a histogram sampling technique.

For the *electron contamination source*, first a uniformly distributed random number r is sampled. If $r < c$ (the weight of the first Gaussian), a position (x, y) is sampled from a 2D-Gaussian with the standard deviation of $\sigma_{\mathrm{e},0}$ — otherwise $\sigma_{\mathrm{e},1}$ is used. The sampling is iterated

until $|x|, |y| < 3\sigma_{e,1}$. The jaw opening visible from each point in the source plane has been pre-calculated into a discretized table. Then for point $\vec{x}_0 = (x, y, 0)$, the corresponding jaw positions are determined. After that, a position $\vec{x}_1 = (x_1, y_1, z_{\mathrm{SAD}})$ is sampled uniformly from the rectangle defined by the jaw positions. Then the same rejection sampling technique as for the primary photon source is used to account for the shape of the fluence profile. The direction is then obtained as $\vec{d} = \vec{x}_1 - \vec{x}_0$, and the particle is projected from $\vec{x}_0$ along $\vec{d}$ to the topmost accessory plane. Finally, the energy E is sampled from $S_{\mathrm{el}}(E)$ using the histogram sampling technique.

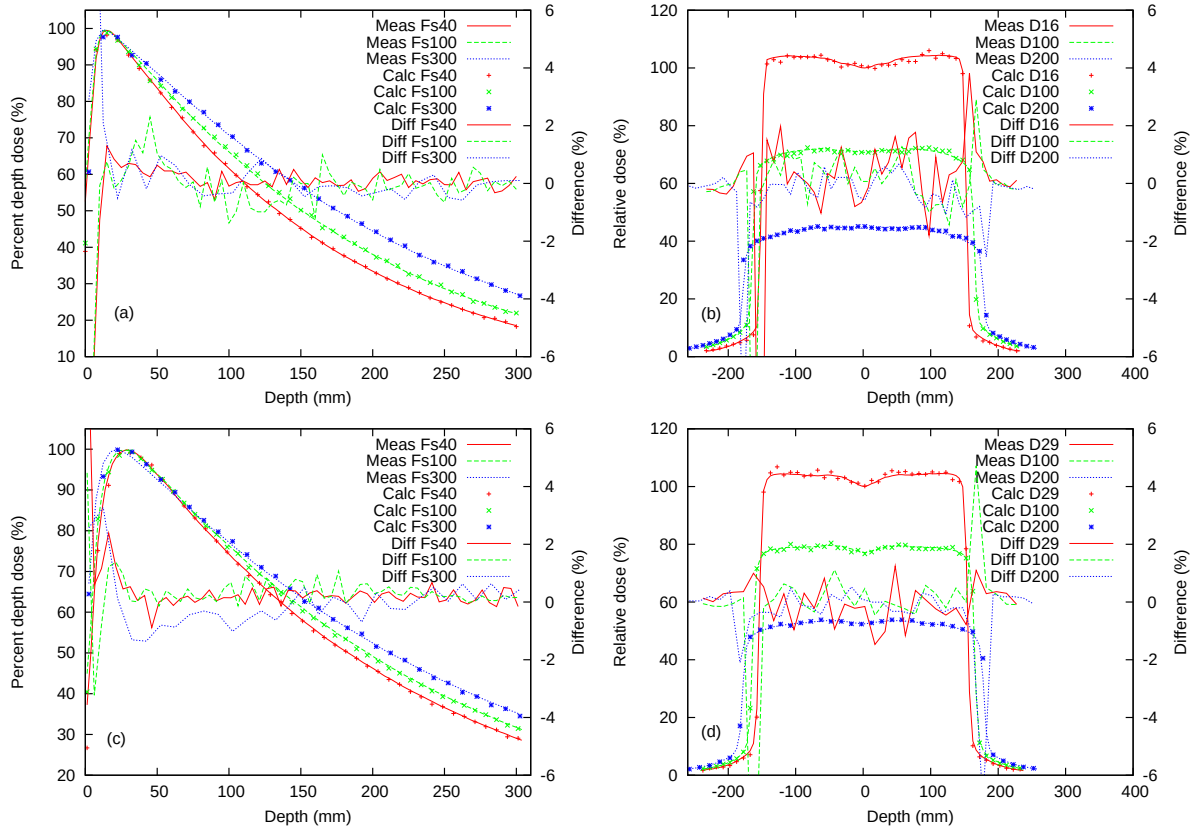

Figure 1. Measured (Meas) and calculated (Calc) open field central axis depth dose curves for 6MV (a) and 15MV (c), and lateral dose profiles for 6MV (b) and 15MV (d), and the corresponding dose differences (Diff). The field size (mm) is indicated in the label after symbol 'Fs' and the depth (mm) after symbol 'D'.

2.5. Transport through static accessories

The secondary collimator jaws are modeled in this work as impenetrable blocks, since the scatter from jaws is included in the extra-focal photon source. Hence, the sampling process described in Section 2.4 is iterated until a particle not hitting the jaws is obtained. Then the particle is transported through all accessories included in the field. The current implementation includes accessory modules for hard wedges, blocks, compensators, and for the Varian 80-leaf MLC. The MLC module accounts for the leaf alignment according to beam divergence, convex and concave leaf structures, two small air cavities between adjacent leaves, and the rounded leaf tip. To reduce the number of boundary checks within the rounded leaf tip, a pair of parallel planes have been added to define the region of the rounded leaf segment [8]. When the intersection of a ray with the MLC module is calculated, the rounded leaf tip needs to be considered only when the intersection point occurs between the parallel planes. For blocks and wedges, the boundary

check problem consists of determining the intersection of rays with planes defined by contour polygons.

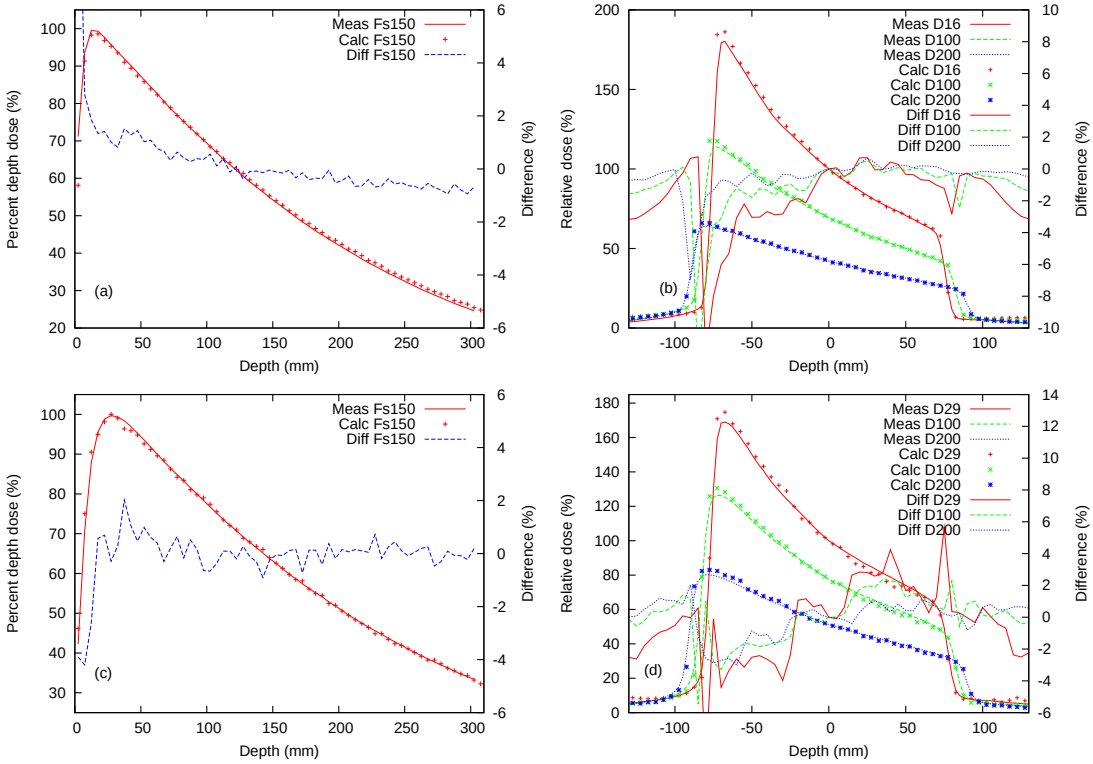

Figure 2. Measured (Meas) and calculated (Calc) central axis depth dose curve for 6MV (a) and 15MV (c), and wedge profiles for 6MV (b) and 15MV (d) for a 60° physical upper wedge, and the corresponding dose differences (Diff).

3. Results and discussion

The developed process was applied to two beam data sets (6MV and 15MV) from a Varian 2100 C/D accelerator. The measurements were conducted at the Helsinki University Central Hospital using the IC15 ionization chamber (Scanditronix-Wellhöfer, Schwarzenbruck, Germany) having a volume of 130 mm^3 and the Wellhöfer Blue Phantom. An average statistical accuracy of 1% was used in the calculations. All measurements were normalized to 100% at field central axis d_{max}. Calculations were normalized to measurements at 100 mm depth for each field size.

Comparison of measured and calculated open field depth dose curves for field sizes 40×40, 100×100 and 300×300 mm^2, and profiles for the 300×300 mm^2 field at depths d_{max}, 100 and 200 mm at SSD = 1000 mm are presented in figure 1. There is an excellent agreement between measurements and calculations for each case. The observed deviations are mostly within 2% of field d_{max}, except near the phantom surface and in the field penumbra region, where the deviations are within 2 mm. Similar comparison for a 150×150 mm^2 field for the 60° upper wedge is presented in figure 2. The obtained accuracy is similar to open fields with the exception of high dose area in the profiles measured at 16 mm or 29 mm depth, where the deviations go up to $\sim$3.5% of field d_{max}. These deviations may be caused by inaccuracies in the wedge material composition, or the missing modeling of the wedge tray into which the wedge is mounted.

The accuracy of the MLC module and absolute dose calibration were tested by comparing measured and calculated absolute point doses for five irregular MLC apertures shown in figure 3. The jaws were fixed to 200×200 mm^2 position for each aperture. The absolute dose corresponding to 100 MUs was measured at 50 mm depth in the position marked with $\times$ in

figure 3 at SSD = 1000 mm. The results of the comparison are shown in table 1. The agreement is excellent for each case, since the maximum error is -1.6% (Arrow, 6MV).

4. Conclusions

This work demonstrates that the developed source model and optimization procedure can be used with VMC++ to obtain accurate dose distributions for open, wedged and static MLC fields. Hence, the developed procedure could be utilized in the future for commissioning the VMC++ algorithm for clinical use in a hospital.

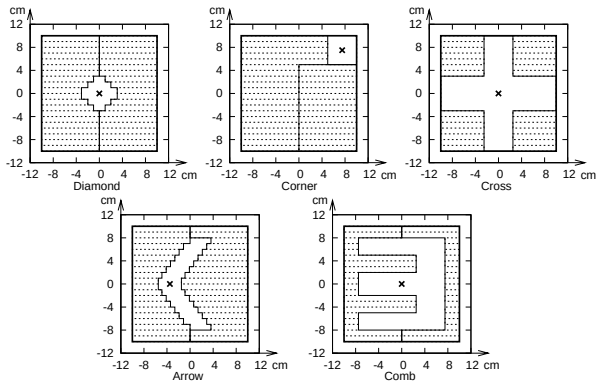

Figure 3. An illustration of the five different MLC apertures (Diamond, Corner, Cross, Arrow and Comb) used in the testing process. The measurement point is marked with × for each MLC aperture.

Table 1. Comparison of measured and calculated absolute point doses for five irregular MLC apertures.

	6MV			15MV		
Aperture	Meas (Gy)	Calc (Gy)	Diff (%)	Meas (Gy)	Calc (Gy)	Diff (%)
Diamond	0.867	0.855	−1.4	0.951	0.952	0.1
Corner	0.895	0.885	−1.1	0.994	0.984	−1.0
Cross	0.933	0.941	0.9	0.993	0.987	−0.6
Arrow	0.893	0.879	−1.6	0.987	0.981	−0.6
Comb	0.905	0.913	0.9	0.975	0.988	1.3

References

[1] Kawrakow I and Fippel M 2000 VMC++, a fast MC algorithm for radiation treatment planning *Proc. XIIIth Int. Conf. on the Use of Computers in Radiation Therapy (Heidelberg)* ed W Hamacher and T Bortfeld (Heidelberg: Springer-Verlag) pp 126–8

[2] Kawrakow I 2001 VMC++, electron and photon Monte Carlo calculations optimized for radiation treatment planning *Proc. of the Monte Carlo 2000 Conference (Lisbon)* ed A Kling, F Barao, M Nakagawa and L Travora (Berlin: Springer)

[3] Verhaegen F, Seuntjens J 2003 Monte Carlo modelling of external radiotherapy photon beams *Phys. Med. Biol.* **48** R107-R164

[4] Sheikh-Bagheri D and Rogers D W O 2002 Sensitivity of megavoltage photon beam Monte Carlo simulations to electron beam and other parameters *Med. Phys.* **29** 379–90

[5] Liu H H, Mackie T R and McCullough E C 1997 A dual source photon beam model used in convolution/superposition dose calculations for clinical megavoltage x-ray beams *Med. Phys.* **24** 1960–71

[6] Fippel M, Haryanto F, Dohm O and Nusslin F 2003 A virtual photon energy fluence model for Monte Carlo dose calculation *Med. Phys.* **30** 301–11

[7] Tillikainen L, Siljamäki S, Helminen H, Alakuijala J and Pyyry J 2007 Determination of parameters for a multiple-source model of megavoltage photon beams using optimization methods *Phys. Med. Biol.* **52** 1441–67

[8] Figini S P, Fix M K, Manser P, Born E J, Frei D, Volken W, Neuenschwander H, Niederer P, Mini R 2003 Towards clinical Monte Carlo treatment planning for photon peams: Swiss Monte Carlo plan *Med. Phys.* **30** 1516